Theor Appl Genet (2014) 127:1537–1547
DOI 10.1007/s00122-014-2317-8

ORIGINAL PAPER

A truncated FatB resulting from a single nucleotide insertion is responsible for reducing saturated fatty acids in maize seed oil

Peizhong Zheng · MD Ali Babar · Seshasai Parthasarathy · Ryan Gibson · Kelly Parliament · Josh Flook · Thomas Patterson · Peter Friedemann · Siva Kumpatla · Steve Thompson

Received: 13 January 2014 / Accepted: 16 April 2014 / Published online: 7 May 2014

Abstract
Key message **We identified a G-nucleotide insertion in a maize *FatB* responsible for reducing saturated fatty acids through QTL mapping and map-based cloning and developed an allele-specific DNA marker for molecular breeding.**
Abstract Vegetable oils with reduced saturated fatty acids have signficant health benefits. SRS72NE, a Dow AgroSciences proprietory maize inbred line, was found to contain signficantly reduced levels of palmitic acid and total saturated fatty acids in seed oil when compared to other common inbreds. Using F_2 and F_3 populations derived from a cross between SRS72NE and a normal inbred SLN74, we have demonstrated that the reduced saturated fatty acid phenotype in SRS72NE is controlled by a single QTL on chromosome 9 that explains 79.1 % of palmitic acid and 79.6 % total saturated fatty acid variations. The QTL was mapped to an interval of 105 kb that contains one single gene, a type B *fatty acyl-ACP thioesterase* (*ZmFatB*; *GRMZM5G829544*). *ZmFatB* alleles from SRS72NE and common inbreds were cloned and sequenced. SRS72NE *fatb* allele contains a single nucleotide (G) insertion in the 6th exon, which creates a premature stop codon 22 base pairs down stream. As a result, ZmFatB protein from SRS72NE is predicted to contain eight altered and 90 deleted amino acids at its C-terminus. Because the affected region is part of the conserved acyl-ACP thioesterase catalytic domain, the truncated ZmFatB in SRS72NE is likely non-functional. We also show that *fatb* RNA level in SRS72NE is reduced by 4.4-fold when compared to the normal allele SNL74. A high throughput DNA assay capable of differentiating the normal and reduced saturate fatty acid alleles has been developed and can be used for accelerated molecular breeding.

Introduction

Vegetable oils with high oleic acid (a monounsaturated fatty acid) content and/or low levels of saturated fatty acids provide considerable health and cooking benefits when compared to saturated and polyunsaturated fatty acids (Kinney et al. 2002; White and Weber 2003). According to the 2010 Dietary Guidelines published by US Department of Agriculture and US Department of Health and Human Services, humans should 'consume <10 % of calories from saturated fatty acids by replacing them with monounsaturated and polyunsaturated fatty acids' (http://health.gov/dietaryguidelines/2010.asp).

Plant fatty acid biosynthesis occurs in the plastids. Towards the end of the biosynthetic pathway, a group of enzymes called acyl-ACP thioesterases (TEs) catalyze the hydrolysis of acyl-ACP thioester bonds to release free fatty acids and acyl carrier proteins. Free fatty acids are then transported to the cytosol, esterified to coenzyme A, and incorporated into membrane lipids or stored as triacylglycerols (TAGs). Plant acyl-ACP TEs can be further classified into two distinct but related families, FatA and FatB. FatAs

Communicated by T. Lubberstedt.

Electronic supplementary material The online version of this article (doi:10.1007/s00122-014-2317-8) contains supplementary material, which is available to authorized users.

P. Zheng (✉) · MD Ali Babar · S. Parthasarathy · R. Gibson · K. Parliament · J. Flook · T. Patterson · P. Friedemann · S. Kumpatla · S. Thompson
Dow AgroSciences LLC, 9330 Zionsville Road, Indianapolis, IN 46268, USA
e-mail: pzheng@dow.com

generally prefer unsaturated fatty acids and have the highest specificity for C18:1-ACP, lower specificities towards C16:1-ACP and C18:0-ACP, and minor activity towards C16:0-ACP. FatBs prefer saturated fatty acids as substrates but some FatBs also have significant specificities for unsaturated acyl-ACPs (Salas and Ohlrogge 2002; Mayer and Shanklin 2007). As a class, FatBs have a broad range of substrate specificities for C8 to C18-ACPs. For examples, FatB1 from *Umbellularia californica* has specific activities towards C12:0-ACP (Davies et al. 1991); the housekeeping FatB1 from *Cuphea hookeriana* has been shown to have activities on C14 to C18 acyl-ACPs, with a strong preference for C16:0-ACP (Jones et al. 1995), whereas the seed-specific FatB2 from the same species displays high specificities on C8:0 and C10:0 acy-ACPs (Dehesh et al. 1996). The substrate preferences of individual acyl-ACP TEs are known to play a key role in determining the fatty acid composition and the ratio of saturated versus unsaturated fatty acids of storage lipids in different plants (Voelker et al. 1992; Jones et al. 1995; Dehesh et al. 1996; Hills 1999).

Commercial corn oil is generally considered a high-quality oil for human consumption because it contains 80.5 % unsaturated fatty acids, mostly consisting of oleic acid (C18:1; 28.3 %) and linoleic acid (C18:2; 50.6 %) and 19.5 % saturated fatty acids, predominantly palmitic acid (C16:0) (Kim et al. 2009; Dauqan et al. 2011). Corn oil is also less susceptible to oxidation because it contains only 1.2 % linolenic acid (C18:3), compared to 7.8 % for soybean oil and 13.0 % for conventional canola oil (White and Weber 2003; Kim et al. 2009; Shen et al. 2010). Maize grains with high oleic acid levels ranging from 50 to 82 % (Wright 1995; Alexander and Jellum 1998; Leto and Ulrich 2004; Shen 2006) as well as varieties with high oleic (64.0 % or greater) and low total saturated fatty acids (TSAT; 5.6 %) and palmitic acid (4.3 %) (Nagel 2005) have been reported, suggesting that there is room for further improvement in the ratio of saturated and unsaturated fatty acids for current commercial corn oil.

Both total oil content and fatty acid composition in corn are known to be complex traits controlled by multiple quantitative trait loci (QTLs). Studies have identified a number of oil content and fatty acid composition QTLs in different mapping populations or diversity panels (Berke and Rocheford 1995; Alrefai et al. 1995; Mangolin et al. 2004; Dudley et al. 2004, 2007; Laurie et al. 2004; Clark et al. 2006; Willmot et al. 2006; Beló et al. 2008; Wassom et al. 2008a, b, Zheng et al. 2008; Wang et al. 2010; Yang et al. 2010, 2012; Cook et al. 2011; Li et al. 2011, 2013; Zhang et al. 2012). A few genes responsible for these QTLs have been cloned and validated, notably *ZmDGAT1-2* controlling oil content and oleic/linoleic ratio (Zheng et al. 2008; Chai et al. 2012), *ZmFAD2* controlling oleic acid concentration (Beló et al. 2008) and *ZmFatB* controlling palmitic acid concentration (Li et al. 2011). DNA markers based on *ZmDGAT1-2* and *ZmFatB* have also been developed for marker-assisted selection and molecular breeding of nutritionally improved maize oil (Chai et al. 2012; Li et al. 2011).

In a survey of seed oils from Dow AgroSciences (DAS) maize inbreds, the inbred SRS72NE was found to contain reduced concentrations of palmitic acids (C16:0) and TSAT when compared to many common inbreds. Here we describe the genetic mapping of the reduced TSAT trait in SRS72NE and the discovery of its underlying gene and mutation.

Materials and methods

Plant material and DNA extraction

SRS72NE is an inbred line developed by DAS breeders through conversional breeding. It contains reduced levels of C16:0 and TSAT. SLN74 is a DAS inbred line with normal saturated fatty acid levels typically found in corn germplasm. F_1 lines were generated by crossing SRS72NE (as a female) and SLN74 (as a male). DNA for genotyping and other molecular experiments was extracted from F_2 and F_3 leaf tissues using a DAS DNA extraction procedure. Seeds from F_3 and F_4 ears derived from self-pollinating F_2 and F_3 plants were used for fatty acid composition analysis.

Single-seed fatty acid methyl ester (FAME) analysis

A single seed was ground and TAGs were extracted with heptane. TAGs were hydrolyzed to glycerol and free fatty acids using 2 M KOH followed by sodium methoxide/methanol transesterification. Samples were then analyzed in a 6890 Series Gas Chromatograph system from Agilent Technologies (Santa Clara, CA) with a DB-23 60-m column (Agilent part number 122-2362) and a flame ionization detector. Methyl ester reference standards were purchased from Nu-Chek-Prep, Inc. (Elysian, MN) and used to identify the fatty acid peaks in each sample. The oven temperature was set at 190 °C and maintained throughout the run. The inlet split ratio was 1:25 and the inlet temperature was 280 °C. Hydrogen carrier gas was set to a flow of 3.0 ml/min for 0.3 min before it was ramped at 0.5 to 4.0 ml/min and held for 15.5 min, before it was dropped to 3.5 ml/min at a rate of 0.5 ml/min and held for the remaining run time. The detector temperature was set at 300 °C with a constant carrier gas make up of 20 ml/min, fuel hydrogen flow of 30 ml/min, and oxidizer flow of 400 ml/min. Empower software from Waters Corporation (Milford, MA) was used to calculate and report the percent areas and concentrations of each test sample. FAME peaks were

identified by comparison to the retention times of the reference standard compounds. The relative fatty acid composition for each sample was calculated by dividing individual peak area by the sum of all the FAME peak areas. TSAT is calculated as the sum of all measurable saturated fatty acids.

KASPar genotyping

KBioscience's (www.kbioscience.co.uk/reagents/KASP/KASP.html) Competitive Allele-Specific Polymerase chain reaction (KASPar) assays were used for SNP genotyping of F_2 and F_3 populations. Assay primers were designed using the Kraken software from KBioscience (Hertfordshire, UK) and synthesized by Integrated DNA Technologies (IDT; Coralville, IA). Assay conditions and reaction setups were according to the recommendations by KBioscience. ABI GeneAmp® PCR System 9700 (Applied Biosystems, Foster City, CA) was used for amplification. PCR cycles started at 94 °C for 15 min, then 20 cycles with 10 s of denature at 94 °C and 5 s of annealing at 57 °C, then 10 s of extension at 72 °C, followed by 22 cycles with 10 s of denature at 94 °C and 20 s of annealing at 57 °C, then 40 s of extension at 72 °C. PCR products were measured by PheraStar spectrofluorometer (BMG LABTECH Inc., Cary, NC) with excitation wavelength at 485 nm and emission wavelength at 520 nm for fluorescent signal of fluorescein amidite (FAM) and 520 and 560 nm for VIC. Genotype calls were made based on the cluster separation in a cluster view using the Kraken software.

QTL mapping

QTL Cartographer 2.5 (Wang et al. 2012b) was used for QTL mapping. The QTL significance level for composite interval mapping was determined by 500 permutations at $P < 0.05$. Genetic positions are based on a DAS maize consensus map. Physical positions are based on B73 RefGen-v2.

ZmFatB cloning and sequencing

ZmFatB forward and reverse PCR primers (sequences listed in Suppl. Table 1) were designed based on B73 inbred *FatB* gene *GRMZM5G829544*. PCR amplification was performed in a BIO-RAD iCycler (Bio-RAD Laboratories, Hercules, CA) in reactions containing 2.5 units of TaKaRa LA Taq™ DNA polymerase (Takara Bio Inc., Shiga, Japan), 400nM of dNTP, 200nM each of forward and reverse primers and 10 ng of genomic DNA. The following PCR program was used: 5 min of denaturing at 94 °C; 30 cycles of 98 °C for 30 s, 65 °C for 15 min; a 10-min extension at 72 °C. PCR products were gel-extracted and purified using QIAquick Gel Extraction Kit from Qiagen (Valencia, CA) and submitted to Eurofins MWG Operon (Huntsville, AL) for direct sequencing.

Gene expression by quantitative real time-PCR (qRT-PCR) assay

Embryos were dissected from immature kernels (20 days after pollination) and total RNA was extracted using the TRIzol® Plus RNA Purification System from Invitrogen (Carlsbad, CA). The cDNA was synthesized using a protocol recommended by SuperScript III First-Strand Synthesis SuperMix for qRT-PCR kit (Invitrogen) and normalized to 10 ng/µl.

A TaqMan assay based on the junction sequence from *ZmFatB* exons 3 and 4 was used to conduct expression studies, with maize *Elongation Factor 1-alpha* (*ZmEF1-A;* GenBank accession number: AF136823) as an internal control for Delta–Delta CT calculation (Livak and Schmittgen 2001). Oligonucleotides for TaqMan assay primers were synthesized by IDT and TaqMan probes were purchased from Life Technologies (sequences listed in Suppl. Table 1). Each qRT-PCR reaction contained 5 µl of 2× Master Mix from Roche Diagnostics (Indianapolis, IN), 0.4 µl of 10 µM forward primer, 0.4 µl of 10 µM reverse primer, 0.4 µl of 5 µM probes, 2.8 µl Milli-Q water, and 1.5 µl of 10 ng/µl cDNA for a total volume of 10.5 µl. *ZmFatB* reactions were carried out in triplicates while the *ZmEF1-A* control was carried out separately as a single reaction. PCR was performed in a Roche LightCycler® 480 II and the relative quantification protocol began with an activation step at 95 °C for 10 min followed by 50 cycles of 95 °C for 10 s, 58 °C for 30 s, and 72 °C for 1 s with a final cooling step at 40 °C for 10 s.

Results

Seed oils from inbred SRS72NE contain reduced palmitic acid and TSAT

To understand natural variations for fatty acid composition in DAS maize germplasm, TAGs from mature maize kernels were extracted from a large panel of DAS inbreds and analyzed for relative concentrations of major fatty acids. Table 1 shows the detailed measurable fatty acid composition of 16 representative DAS inbreds, including SRS72NE. Among these 16 inbreds, significant variations are found for palmitic acid (C16:0), stearic acid (C18:0), oleic acid (C18:1), linoleic acid (C18:2), linolenic acid (C18:3) and arachidic acid (C20:0). The inbred SRS72NE stands out because it has the lowest levels of C16:0 (5.94 %), C20:0 (0.31 %), one of the lowest levels of C18:0 (1.77 %) and

Table 1 Fatty acid composition (%) of 16 DAS inbreds

Inbred	TSAT	C14:0	C16:0	C16:1	C18:0	C18:1	C18:2	C18:3	C20:0	C20:1	C22:0	C24:0
SRS72NE	8.3 ± 0.4	0.03 ± 0.0	5.9 ± 0.1	0.1 ± 0.003	1.8 ± 0.1	28.5 ± 1.8	60.6 ± 1.7	0.9 ± 0.05	0.3 ± 0.02	0.3 ± 0.01	0.1 ± 0.004	0.2 ± 0.01
SLN74	15.1 ± 0.5	0.04 ± 0.0	12.6 ± 0.4	0.2 ± 0.01	1.8 ± 0.2	29.6 ± 4.3	52.3 ± 4.0	1.6 ± 0.1	0.4 ± 0.01	0.3 ± 0.01	0.1 ± 0.01	0.1 ± 0.05
DASIB-1	13.6 ± 0.4	0.05 ± 0.0	10.8 ± 0.2	0.1 ± 0.01	1.9 ± 0.1	28.2 ± 1.5	55.6 ± 1.5	0.9 ± 0.02	0.4 ± 0.02	0.3 ± 0.02	0.1 ± 0.01	0.2 ± 0.01
DASIB-2	14.8 ± 0.3	0.09 ± 0.01	12.1 ± 0.2	0.1 ± 0.02	1.7 ± 0.1	27.6 ± 1.1	52.7 ± 0.7	1.4 ± 0.1	0.5 ± 0.03	0.3 ± 0.03	0.2 ± 0.05	0.2 ± 0.04
DASIB-3	14.4 ± 0.3	0.02 ± 0.005	10.7 ± 0.3	0.1 ± 0.01	2.9 ± 0.2	47.9 ± 1.0	35.8 ± 0.7	0.4 ± 0.02	0.5 ± 0.03	0.3 ± 0.01	0.1 ± 0.01	0.1 ± 0.01
DASIB-4	14.0 ± 0.3	0.03 ± 0.05	10.8 ± 0.3	0.1 ± 0.01	2.5 ± 0.1	47.1 ± 0.6	36.8 ± 0.6	0.4 ± 0.01	0.5 ± 0.01	0.3 ± 0.01	0.1 ± 0.005	0.1 ± 0.01
DASIB-5	16.7 ± 0.3	0.03 ± 0.0	14.0 ± 0.3	0.1 ± 0.01	2.1 ± 0.1	37.1 ± 0.9	43.8 ± 0.9	0.4 ± 0.01	0.4 ± 0.02	0.3 ± 0.01	0.1 ± 0.004	0.1 ± 0.01
DASIB-6	12.6 ± 0.7	0.03 ± 0.003	9.9 ± 0.5	0.1 ± 0.01	2.0 ± 0.3	39.8 ± 1.0	45.3 ± 0.7	0.6 ± 0.02	0.5 ± 0.04	0.3 ± 0.02	0.1 ± 0.01	0.1 ± 0.01
DASIB-7	12.4 ± 0.2	0.03 ± 0.0	9.3 ± 0.1	0.1 ± 0.003	2.3 ± 0.1	38.3 ± 1.2	47.0 ± 1.1	0.8 ± 0.03	0.5 ± 0.02	0.2 ± 0.01	0.1 ± 0.01	0.1 ± 0.01
DASIB-8	14.0 ± 0.4	0.05 ± 0.01	11.4 ± 0.6	0.1 ± 0.01	1.8 ± 0.2	29.8 ± 1.9	53.7 ± 1.9	0.9 ± 0.1	0.4 ± 0.03	0.3 ± 0.02	0.1 ± 0.01	0.2 ± 0.02
DASIB-9	14.6 ± 0.1	0.03 ± 0.005	11.5 ± 0.1	0.1 ± 0.01	2.4 ± 0.2	34.8 ± 0.5	48.1 ± 0.5	0.5 ± 0.02	0.5 ± 0.02	0.3 ± 0.01	0.1 ± 0.01	0.1 ± 0.005
DASIB-10	16.1 ± 0.2	0.03 ± 0.0	12.9 ± 0.1	0.1 ± 0.01	2.4 ± 0.1	38.5 ± 0.9	43.4 ± 0.8	0.5 ± 0.02	0.5 ± 0.02	0.3 ± 0.02	0.1 ± 0.01	0.1 ± 0.01
DASIB-11	16.4 ± 0.3	0.04 ± 0.0	13.4 ± 0.4	0.1 ± 0.004	2.2 ± 0.1	41.1 ± 2.2	40.2 ± 2.1	0.6 ± 0.03	0.5 ± 0.01	0.3 ± 0.01	0.1 ± 0.01	0.1 ± 0.01
DASIB-12	12.7 ± 0.3	0.05 ± 0.01	9.8 ± 0.3	0.1 ± 0.01	2.1 ± 0.3	29.5 ± 2.4	54.3 ± 2.4	1.5 ± 0.1	0.4 ± 0.02	0.2 ± 0.02	0.1 ± 0.01	0.2 ± 0.04
DASIB-13	13.0 ± 0.2	0.04 ± 0.0	10.2 ± 0.2	0.1 ± 0.01	2.1 ± 0.1	27.0 ± 1.5	57.5 ± 1.4	1.0 ± 0.02	0.4 ± 0.02	0.2 ± 0.01	0.1 ± 0.01	0.2 ± 0.01
DASIB-14	13.3 ± 0.4	0.06 ± 0.01	10.5 ± 0.3	0.1 ± 0.01	1.9 ± 0.1	27.4 ± 1.5	56.3 ± 1.8	1.0 ± 0.04	0.5 ± 0.03	0.3 ± 0.01	0.2 ± 0.01	0.2 ± 0.01

Data represent averages of five kernels with standard deviations

consequently, the lowest level of TSAT (8.34 %). C16:0 and TSAT concentrations in SRS72NE are reduced by 58.5 % (student's *T* test $P = 6.3E{-}12$) and 50.1 % ($P = 1.8E{-}10$) respectively when compared to DASIB-5, the inbred with the highest levels of C16:0 and TSAT; and by 35.6 % ($P = 5.1E{-}10$) and 32.5 % ($P = 3.0E{-}10$) respectively when compared to DASIB-7, the inbred that contains the 2nd lowest levels C16:0 and TSAT (Table 1).

The reduced TSAT phenotype in SRS72NE is controlled by a single QTL

Because SRS72NE has such a large reduction in saturated fatty acids, the genetic basis of the phenotype was further investigated through QTL mapping. A database search revealed that several F_2 seed sources with SRS72NE as one of the parents were available in DAS, including the cross between SRS72NE and SLN74, an inbred line containing normal levels of saturated fatty acids (Table 1).

In the summer of 2010, 309 SRS72NE x SLN74 F_2 plants were grown in Sydney, IL and self-pollinated to produce F_3 ears. DNA was extracted from F_2 leaf tissues and genotyped with 133 polymorphic SNP markers evenly distributed on 10 chromosomes. Five kernels from each F_3 ear were subjected to single-kernel FAME analysis. The five-kernel average values for TSAT and individual fatty acid species were used as the ear phenotypic data for QTL mapping. Because the concentrations for C14:0, C16:1, C20 and longer chain length fatty acids are very low in corn oil and the measurement accuracy may not be reliable, QTL mapping was performed for TSAT, C16:0, C18:0, C18:1, C18:2 and C18:3 only.

As shown in Fig. 1a, there is a very strong QTL for both TSAT and C16:0 traits in the same region on chromosome 9 and the logarithm of odds (LOD) score plots for both traits are almost completely overlapped. No other significant QTLs for C16:0 or TSAT were detected in the genome. The QTLs for TSAT and C16:0 on chromosome 9 explain 79.05 and 79.55 % phenotypic variations (R^2) respectively in the F_2 population (Table 2). One allele additive effects (A) for TSAT and C16:0 concentrations are 2.56 and 2.81 % respectively, with the SRS72NE allele decreasing the traits.

In addition to QTLs with very large LOD scores for TSAT and C16:0, the same or similar genetic interval also contains significant QTLs for all species of C18 fatty acids. In contrast to reducing C16:0 and TSAT, the SRS72NE allele significantly increases C18:0, C18:1 and C18:2 fatty acid concentrations, with a single allele additive effects of 0.19, 0.92 and 1.47 % respectively (Table 2). In fact, the combined increases in C18:0, C18:1 and C18:2 explain 91.8 % of the C16:0 percentage reduction. The SRS72NE allele from this genetic interval also appears to slightly reduce C18:3. The R^2 values for C18:0, C18:1, C18:2 and

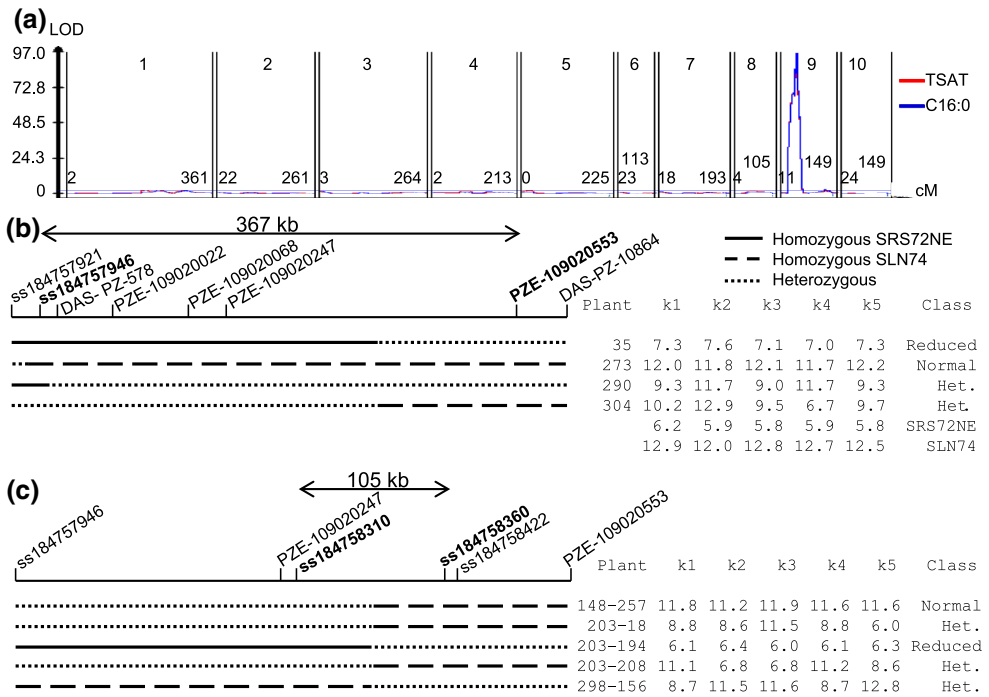

Fig. 1 QTL mapping of TSAT and C16:0 traits on chromosome 9. **a** LOD plot for TSAT and C16:0 traits in F_2. Chromosome numbers are labeled on the top, first and last marker positions for each chromosome are labeled at the bottom of the panel. **b**, **c** QTL fine mapping in $F_{2:3}$ and $F_{3:4}$ respectively showing genotypic and C16:0 phenotypic data for the most informative recombinants. Markers defining the QTL intervals are in bold and the physical distances of the QTL intervals are indicated. Not all markers used in the study are shown. Precise locations of crossovers are not known and are designated at the midpoint between two adjacent markers

Table 2 Chromosome 9 fatty acid QTL statistics

Trait	Peak (cM)	Interval (cM)	LOD	*A* (%)[a]	R^2 (%)
TSAT	48.05	25.40–58.50	90.05	−2.56	79.05
C16:0	48.05	25.40–58.50	96.42	−2.81	79.55
C18:0	48.55	25.40–63.20	33.12	0.19	34.37
C18:1	46.05	25.80–58.50	5.76	0.92	6.04
C18:2	43.97	25.80–54.60	11.61	1.47	11.95
C18:3	53.18	48.10–58.20	2.98	−0.02	1.93

[a] Additive effect. Negative values indicate that SRS72NE allele decreases the trait

C18:3 are 34.47, 6.04, 11.94 and 1.93 % respectively, much lower than those for TSAT and C16:0 (Table 2). Consistently, we have also detected 5, 10, 7 and 5 additional significant QTLs in other genomic regions for C18:0, C18:1, C18:2 and C18:3 traits respectively (data not shown).

TSAT QTL mapped to a 105-kb interval

Since approximately 80 % of TSAT consisted of palmitic acids in our mapping population and the QTL peak positions for C16:0 and TSAT on chromosome 9 are identical (Table 2), we decided to mainly focus on the C16:0 QTL, which has a somewhat larger additive effect, for fine mapping and other studies going forward. We also suspected that C16:0 concentrations in the F_3 ears would phenotypically show distinct classes depending on how many SRS72NE alleles of the chromosome 9 QTL each plant inherited since the QTL explained ~80 % of the phenotypic variations. To confirm, we examined C16:0 data for the five individual kernels from each of the 309 F_3 ears used for QTL mapping and found indeed it was the case.

In the examples shown in Fig. 1b, C16:0 concentrations for the five individual kernels (k1–k5) from the F_3 ear derived from plant #35 are more similar to the SRS72NE parent and show little variation, whereas those of ear #273 are more similar to the SLN74 parent and do not appear to segregate. On the other hand, C16:0 concentrations for the five kernels from ears 290 and 304 appear to segregate. For ear 304, the five kernels appear to segregate for three classes: k2 similar to the SLN74; k4 similar to SRS72NE; k1, k3 and k5 similar to the average value of the two parents. For ear 290, C16:0 concentrations for k2 and k4 are similar to SLN74, whereas k1, k3 and k5 are close to the average value of the two parents. C16:0 data for all 309 F_3 ears were carefully investigated. As a result, we were able to classify all ears into one of the three phenotypic classes, homozygous for SRS72NE (reduced) or SLN74 (normal)

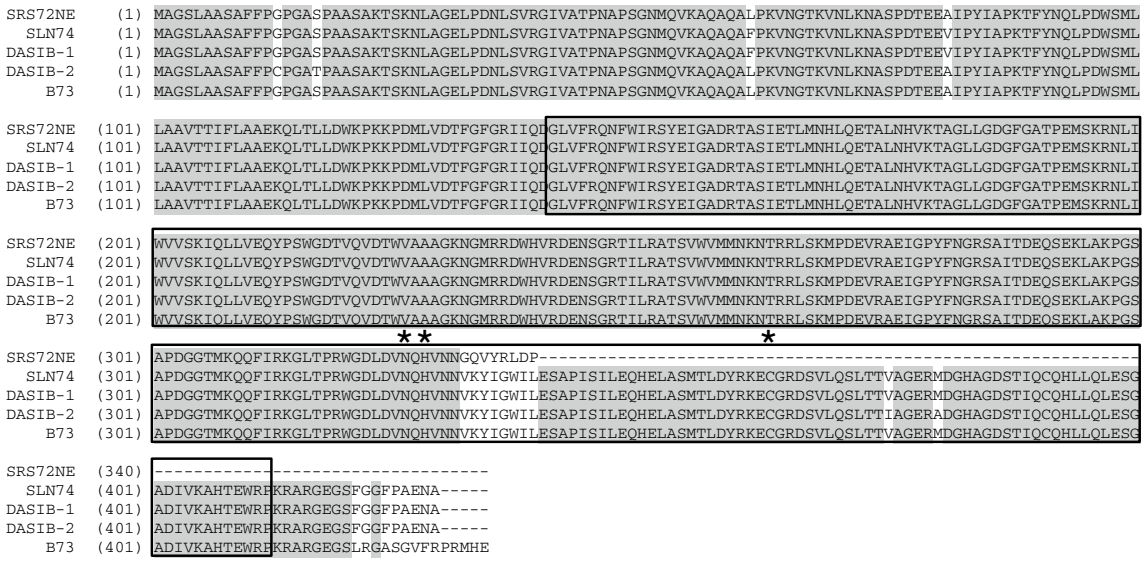

Fig. 2 Sequence alignment of predicted maize FatB proteins. Sequences identical in all alleles are shaded. The conserved acyl-ACP_thioesterase domain is boxed. The three critical catalytic residues (Asn, His and Cys) are labeled with a *asterisk*

and segregating (heterozygous), though in some heterozygous ears, not all three phenotypic classes were present in the initial five kernels analyzed (e.g., ear 290 above).

In the next step, all recombinant F_2 plants within the C16:0 QTL interval on chromosome 9 (25.4–58.5 cM) were identified and genotyped with an additional 52 SNP markers concentrating on the QTL interval. By comparing the genotypic data of these recombinant F_2 plants and their corresponding F_3 single-seed C16:0 concentrations, the TSAT QTL on chromosome 9 was mapped to a much smaller region. Figure 1b shows genotypic and phenotypic data for the four most informative recombinant F_2 plants/F_3 ears. The TSAT QTL is defined within the flanking SNP markers ss184757946 and PZE-109020553. According to maize B73 RefGen_v2, this interval is approximately 367 kb (Fig. 1b) and contains 13 predicted genes.

To map the TSAT QTL on chromosome 9 further, seeds from 10 F_3 ears still segregating for the QTL interval were planted in 2011 summer nursery to generate a large mapping population of 2,460 F_3 plants. Additional 12 SNP-based KASPar markers were also developed within the 367-kb region previously defined in the F_2. Six KASPar markers, between ss184757946 and PZE-109020553 (Fig. 2b), were used to genotype all 2,460 F_3 plants. As a result, 73 recombinants within the 367-kb region were identified. These plants were then genotyped by the 12 newly developed KASPar markers to further refine the recombination point for each plant. All 73 plants were also self-pollinated to produce F_4 ears and the resulting F_4 seeds were subjected to single-seed FAME analysis.

By comparing genotypic data of the recombinant F_3 plants and their corresponding F_4 ear C16:0 data, the TSAT QTL on chromosome 9 was further narrowed down. Figure 1c shows the genotypic and phenotypic data for the five most informative recombinant F_3 plants/F_4 ears. The TSAT QTL is defined by SNP markers ss184758310 (chromosome 9 physical position 20,488,597) and ss184758360 (physical position 20,593,557), or approximately 105 kb according to B73 RefGen_v2 (Fig. 1c).

A closer examination of this genomic region in B73 genome (www.maizesequence.org) reveals that the 5′ end 94.4 kb largely consists of repetitive sequences. The remaining 10.6-kb non-repetitive sequence contains only one gene, *GRMZM5G829544*, which is predicted to encode a protein highly homologous to plant type B fatty acyl-ACP thioesterases (FatB). The predicted GRMZM5G829544 protein sequence is 92 % identical to a *Sorghum bicolor* FatB (EER87824) that has specificities towards C14:0, C16:0 and C16:1-ACPs (Jing et al. 2011); 68 % identical to an *Elaeis guineensis* (African oil palm, AAD42220) and two *Cocos nucifera* (coconut) FatBs (AEM72519 and AEM72520) that prefer C14:0 and C16:1-ACP as substrates (Jing et al. 2011); 60, 58, 57 and 55 % identical respectively to FatBs with strong preferences for C16:0-ACP from *Jatropha curcas* (ABU96744) (Wu et al. 2009), *C. hookeriana* (FatB1, Q39513) (Jones et al. 1995), *Arabidopsis thaliana* (CAA85388) (Bonaventure et al. 2003; Belide et al. 2012) and *Gossypium hirsutum* (cotton, AAF22015) (Pirtle et al. 1999). Therefore, the *ZmFatB* located in the mapping interval was identified as a strong candidate gene responsible for the reduced TSAT phenotype in SRS72NE. Since the TSAT QTL has the largest effect on C16:0 (Table 2), it is likely that the gene product encoded by this *ZmFatB* is a palmitoyl-ACP thioesterase (PATE) that prefers C16:0-ACP as a substrate.

SRS72NE *fatb* contains a single nucleotide (G) insertion

To confirm that *GRMZM5G829544* (*ZmFatB*) is the gene responsible for the TSAT phenotype in SRS72NE, the genomic sequences of this gene were amplified by PCR. Primers were designed so that a 3.6-kb fragment covering the coding region and some additional 5′ and 3′-UTR sequences could be amplified. The primer pair successfully amplified *ZmFatB* from both mapping parents as well as two other DAS inbreds (DASIB-1 and DASIB-2) with normal saturated fatty acid profiles (Table 1). Sequences for all four alleles were completely determined by direct sequencing of the PCR products.

As shown in Suppl. Fig. 1, a total of 108 polymorphic sites (57 located in the introns), including SNPs and insertions/deletions (InDels) can be identified when the four *ZmFatB* alleles from this study are compared with the B73 allele. Notably, SRS72NE allele (GenBank accession number KJ676470) contains a single G-nucleotide insertion (nucleotide position 2,547 according to SRS72NE sequence; between 20,587,349 and 50 bp in B73 RefGen_v2) in exon 6 (exon #5 in Suppl. Fig. 1 because exon 1 of *ZmFatB* is further upstream and not part of the amplified sequences). This G-nucleotide is absent in SNL74 (KJ676471), DASIB-1 (KJ676472), DASIB-2 (KJ676473) and B73 sequences.

Because the G-nucleotide insertion in SRS72NE *fatb* is located within an exon, it creates a frame-shift and a stop codon 22 bp downstream of the insertion (Suppl. Fig. 1). As a result, FatB protein from SRS72NE is predicted to contain eight altered amino acids (AA) and a deletion of at least 90 AA at its C-terminus (Fig. 2). The altered and deleted regions in SRS72NE FatB are located in the conserved Acyl-ACP_thioesterase domain (Pfam: PF01643 or InterPro: IPR002864) (Fig. 2). Three amino acids (Asn, His and Cys) within the conserved domain have been identified as the critical residues that form a papain-like catalytic triad for *Arabidopsis* and other plant acyl-ACP thioesterases (Yuan et al. 1996; Mayer and Shanklin 2005). These catalytic residues (Asn-326, His-328 and Cys-363 in Fig. 2) are also conserved in the full-length maize FatB. However, Cys-363, which is conserved in all plant FatB proteins, is missing in the truncated SRS72NE FatB due to early termination resulted from the G-insertion (Fig. 2). Consequently, FatB protein from SRS72NE is most likely non-functional even if it is made in the plant.

In addition to the G-insertion polymorphism, there are four other polymorphic sites upstream that also result in AA changes. However, none of these changes is correlated with the reduced TSAT phenotype since FatBs from one or more of the inbreds with normal levels of saturated fatty acids also contain the same AA found in SRS72NE FatB sequence in all four positions (Fig. 2). Therefore, the single nucleotide G-insertion is the causal molecular mutation responsible for reducing TSAT and C16:0 in SRS72NE.

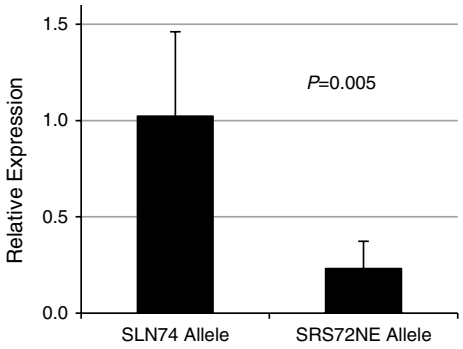

Fig. 3 Relative expression levels of *ZmFatB* RNA determined by qRT-PCR. Data represent the averages of five F_4 ears homozygous for SRS72NE or SLN74 allele but all derived from the same F3 ear. *Error bars* represent standard deviation. *P* value is generated by Student's *T* test

fatb RNA level in SRS72NE is significantly reduced

To determine whether the G-insertion in SRS72NE *fatb* affects its RNA expression, immature ears (20 days after pollination) were harvested from self-pollinated F_4 progenies derived from a single F_3 ear (F_3 ear #53) still segregating for *ZmFatB* on chromosome 9. Embryos were dissected from F_4 ears homozygous for the SRS72NE allele or SLN74 allele at the *ZmFatB* locus as determined by multiple KASPar markers within the 367-kb TSAT QTL interval. Total RNA was extracted from the embryos and *ZmFatB* levels were compared using qRT-PCR as described in "Materials and methods". As shown in Fig. 3, *fatb* RNA expression level in embryos containing the mutated SRS72NE allele with a G-insertion is reduced by 4.4-fold or 77.3 % when compared to that of embryos having the wild type SLN74 allele. These results provide further support that *ZmFatB* on chromosome 9 is the underlying gene for the reduced TSAT phenotype in SRS72NE.

ZmFatB specific high throughput assay for molecular breeding

Since the G-insertion in the *ZmFatB* gene on chromosome 9 was identified as the molecular basis for the reduced TSAT trait in maize inbred SRS72NE, it is now possible to quickly move this trait into any desired maize germplasm through introgression or other molecular breeding approaches using DNA markers. In the TSAT trait mapping process, 70 KASPar assays were developed and validated for the QTL interval (25.4–58.5 cM) and they can be directly used for molecular breeding applications.

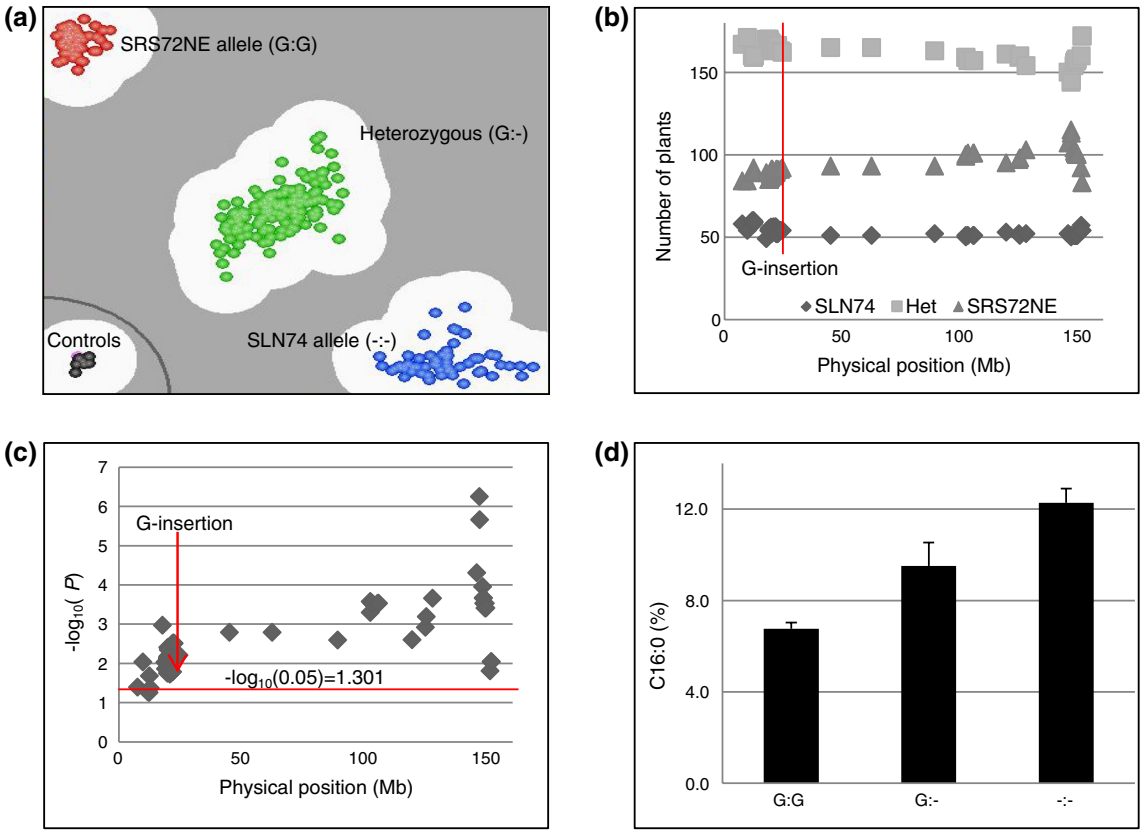

Fig. 4 *ZmFatB* functional KASPar assay and segregation distortion. **a** Genotype calls for the 309 F_2 plants based on the cluster separation using the Kraken software from KBioscience. **b** Number of plants for homozygous SLN74, heterozygous (Het) or homozygous SRS72NE allele for 83 markers on chromosome 9. Position of the G-insertion is indicated. **c** The $-\log_{10}$(*Chi* square test *P* value) for each of the 83 chromosome 9 markers. Positions for the G-insertion and $-\log_{10}(P = 0.05)$ are indicated. **d** Average C16:0 concentrations for three genotype classes. *Error bars* represent standard deviation

Furthermore, an additional 63 SNPs and 15 InDels within the *ZmFatB* gene have been identified between SRS72NE and SLN74 alleles (Suppl. Fig. 1). These markers have not been used for QTL mapping in this study, but they could be converted to KASPar, TaqMan or any other applicable high throughput DNA assays and used to accelerate breeding processes. A high throughput functional marker/assay based on the causal G-insertion would be particularly useful since it detects the molecular basis of the reduced TSAT trait. For this purpose, the G-insertion variation was successfully converted into a KASPar assay (primer sequences listed in Suppl. Table 1) and used to genotype the 309 F_2 plants in this mapping population for validation.

As shown in Fig. 4a, the G-insertion-based KASPar assay is capable of differentiating the three genotypic classes expected in a segregating F_2 population. Among the 309 F_2 plants, 87 are homozygous for SRS72NE allele (G:G), 167 are heterozygous (G:-) and 55 are homozygous for SNL74 allele (-:-). Interestingly, this segregation ratio significantly deviates (*Chi* square test $P = 0.01$) from a typical 1:2:1 ratio expected in an F_2 population. The segregation distortion is not due to assay quality issues associated with the functional KASPar marker since the observed C16:0 and TSAT phenotypes for all 309 F_3 ears match the phenotypes predicted by the marker. Furthermore, none of the 83 markers on chromosome 9 used in this study segregates in 1:2:1 ratio in the F_2 population. As shown in Fig. 4b, all 83 markers are distorted towards having more individuals homozygous for SRS72NE parent than for homozygous SLN74. The peak of distortion is located at 146,529,475 bp (117.24 cM) with a *Chi* square test *P* value of 5.6E−07 (Fig. 4c). These results indicate that the segregation distortion observed is real and the entire chromosome 9 segregates abnormally in the F_2 population.

The average C16:0 concentrations for the three genotypic classes as determined by the functional KASPar marker are 6.76, 9.52 and 12.28 % respectively for homozygous SRS72NE allele, heterozygous and homozygous SLN74 allele, and vary significantly from one another

(Fig. 4d). The *P* values for pair-wise student's *T* test on C16:0 concentrations are 3.66E−112 between G:G and -:- genotypes; 1.23E−67 between G:G and G:- and 8.57E−50 between G:- and -:- respectively. These results further support the earlier conclusion that the G-insertion in *ZmFatB* is responsible for the reduced TSAT trait observed in the inbred SRS72NE.

Discussion

In this study, a maize inbred line (SRS72NE) containing reduced TSAT in its seed oils has been characterized. Using molecular markers and an accurate single-seed FAME phenotyping method, the reduced TSAT trait has been mapped to a *ZmFatB* gene on chromosome 9 and the causal mutation has been identified as a single-nucleotide (G) insertion in its 6th exon in the SRS72NE allele. The insertion creates a frame-shift and is predicted to result in a truncated, non-functional PATE or FatB protein.

Only a single significant QTL for C16:0 and TSAT is detected in the SRS72NE × SLN74 $F_{2:3}$ population used in this study. The result is somewhat surprising considering others have reported multiple QTLs for C16:0 in their mapping populations (Alrefai et al. 1995; Yang et al. 2010). This could be due to the lack of diversity in genetic loci controlling C16:0 between the two mapping parents we used, with the exception of *ZmFatB* locus on chromosome 9. It could also be due to the overwhelming effect from the *FatB* locus (R^2 = 79.55 %) on chromosome 9 that makes detection of other minor C16:0 QTLs in our mapping population difficult. In comparisons, four RFLP loci associated with C16:0 only explain 24.0 % of the total phenotypic variation in the Illinois High Oil by Illinois Low Oil F_2S_1 population (Alrefai et al. 1995) and the most significant C16:0 QTL only accounts for 42.0 % of the total variation in the B73 by Beijing High Oil $F_{7:8}$ RIL population (Yang et al. 2010).

In addition to reducing palmitic acids and TSAT, the mutated *fatb* allele from SRS72NE also appears to be responsible for increasing 18:0, C18:1 and C18:2 concentrations. Palmitic acid is a key intermediate in fatty acid biosynthesis. With a predicted non-functional PATE, less free C16:0 is expected to be available for incorporation into storage lipids in the seed of SRS72NE. Consequently, there is more C16:0-ACP available for 3-ketoacyl-ACP synthase II to make C18:0-ACP, which in turn is converted to unsaturated 18-carbon fatty acyl-ACP. Consistent with these predictions, we have observed dramatically decreased C16:0 and TSAT and significantly increased C18:0, C18:1 and C18:2 fatty acid concentrations contributed by the *ZmFatB* region from SRS72NE allele in our mapping population. Because each SRS72NE allele only increases C18:0 by 0.19 % but decreases 16:0 by 2.81 %, the final effect on TSAT is still a dramatic reduction (Table 2). SRS72NE allele also appears to slightly (0.02 %) but significantly reduce C18:3. Given that C18:3-ACP is produced from C18:2-ACP by the desaturase FAD3, an increase in C18:3 concentration by SRS72NE allele is expected. If the reduction in C18:3 observed is also a result of a non-functional ZmFatB, its mechanism is not understood. It is possible that the reduction is not due to *fatb* but another gene in this region for which the SNS72NE allele has a larger decreasing effect on C18:3 than the increasing effect from *fatb*.

The mutation in SRS72NE *fatb* also significantly reduces its RNA level in the developing embryos. This reduction is most likely due to RNA degradation mediated by the frame-shift mutation resulted from the G-insertion in SRS72NE allele that creates a premature, non-functional ZmFatB protein, a mechanism well known in plants and other species (Conti and Izaurralde 2005; Chen et al. 2012).

The finding that a frame-shift mutation in a *ZmFatB* gene is responsible for the reduced TSAT trait is consistent with results recently published by Li et al. (2011). In their study, the authors combined linkage and association mapping to fine map a C16:0 QTL on chromosome 9 initially reported by Yang et al. (2010) and identified an 11-bp insertion (Suppl. Fig. 1; nucleotide position 3,104–3,114 according to B73 genomic sequence) near the 3′end of the same *ZmFatB* gene in B73 allele as the causal variation. However, the B73 allele has a much smaller effect than the SRS72NE allele we identified. For their effects on C16:0 for example, the one allele additive effect (A), R^2 and LOD for SRS72NE allele are −2.81, 79.55, 94.62 versus −1.28, 28 and 9.10 % for the B73 allele in Li's $BC_1S_{1:2}$ population (Li et al. 2011). The differences between the two alleles are likely due to the fact that B73 FatB contains AA changes that are outside of the conserved acyl-ACP_thioesterase domain (Fig. 2), whereas the changes in SRS72NE allele likely make the protein non-functional. The remaining level of C16:0 observed in SRS72NE is likely the result of multiple copies of *ZmFatB* genes in the maize genome. For example, there is another *ZmFatB* gene (*GRMZM2G007489*) on maize chromosome 6 (nucleotide 71,230,196–71,235,013 bp) that shares very high degrees of homology (88 % identical at AA level) with the *ZmFatB* gene on chromosome 9. Together, results from this study and those of Li et al. (2011) demonstrate that *ZmFatB* plays a crucial role in regulating maize saturated fatty acid concentration and is a promising target for maize oil improvement.

To accelerate marker-assisted breeding of reduced TSAT corn, a high throughput functional KASPar assay based on the G-nucleotide insertion in SRS72NE allele has been developed. This assay has been shown to successfully differentiate the mutant and the wild type alleles.

Significant segregating distortion has been observed in the F_2 population for all chromosome 9 markers used in this study with the peak of distortion at 146,529,475 bp. It is not known whether the distortion is due to the reduced TSAT trait or some other factors. Segregation distortion in maize has been widely reported and a number of consensus segregation distortion regions (SDRs) have been identified (Lu et al. 2002; Yan et al. 2003, Wang et al. 2012a), including those in bin 9.02 and 9.07, near the G-insertion within *ZmFatB* and the peak of distortion, respectively (Fig. 4b, c). However, it would be of scientific interest to investigate why chromosome 9 distortion occurs in our F2 mapping population, it is clearly not the scope of this study.

Acknowledgments The authors would like to thank Tiffiny King for assistance in DNA and RNA sample preparation, Jafar Mammadov and David Meyer for supporting this project.

Conflict of interest The authors declare that they have no conflict of interest.

Ethical standards The experiments in this paper comply with the current laws of the United States.

References

Alexander WL, Jellum MD (1998) Corn oil. European Patent EP0491938

Alrefai R, Berke TG, Rocheford TR (1995) Quantitative trait locus analysis of fatty acid concentration in maize. Genome 38:894–901

Belide S, Petrie JR, Shrestha P, Singh SP (2012) Modification of seed oil composition in Arabidopsis by artificial microRNA-mediated gene silencing. Front Plant Sci 3:168

Beló A, Zheng P, Luck S, Shen S, Meyer DJ, Li B, Tingey S, Rafalski A (2008) Whole genome scan detects an allelic variant of *fad2* associated with increased oleic acid levels in maize. Mol Genet Genomics 279:1–10

Berke TG, Rocheford TR (1995) Quantitative trait loci for flowering, plant ear height and grain traits in maize. Crop Sci 35:1542–1549

Bonaventure G, Salas JJ, Pollard MR, Ohlrogge JB (2003) Disruption of the *FATB* gene in Arabidopsis demonstrates an essential role of saturated fatty acids in plant growth. Plant Cell 15:1020–1033

Chai Y, Hao X, Yang X, Allen WB, Li J, Yan J, Shen B, Li J (2012) Validation of DGAT1-2 polymorphisms associated with oil content and development of functional markers for molecular breeding of high-oil maize. Mol Breed 29:939–949

Chen W, VanOpdorp N, Fitzl D, Tewari J, Friedemann P, Greene T, Thompson S, Kumpatla S, Zheng P (2012) Transposon insertion in a *cinnamyl alcohol dehydrogenase gene* is responsible for a *brown midrib1* mutation in maize. Plant Mol Biol 80:289–297

Clark D, Dudley JW, Rocheford TR, Ledeaux JR (2006) Genetic analysis of corn kernel chemical composition in the random mated 10 generations of the cross of generations 70 of IHO × ILO. Crop Sci 46:807–819

Conti E, Izaurralde E (2005) Nonsense-mediated mRNA decay: molecular insights and mechanistic variations across species. Curr Opin Cell Biol 17:316–325

Cook JP, McMullen MD, Holland JB, Tian F, Bradbury P, Ross-Ibarra J, Buckler ES, Flint-Garcia SA (2011) Genetic architecture of maize kernel composition in the nested association mapping and inbred association panels. Plant Physiol 158:824–834

Dauqan EMA, Sani HA, Abdullah A, Kasim ZM (2011) Fatty acid composition of four different vegetable oils (red palm olein, palm olein, corn oil and coconut oil) by gas chromatography. In: 2nd international conference on chemistry and chemical engineering, IPCBEE, vol 14, pp 31–34

Davies HM, Anderson L, Fan C, Hawkins DJ (1991) Developmental induction, purification, and further characterization of 12:0-ACP thioesterase from immature cotyledons of *Umbellularia californica*. Arch Biochem Biophys 290:37–45

Dehesh K, Jones A, Knutzon DS, Voelker TA (1996) Production of high levels of 8:0 and 10:0 fatty acids in transgenic canola by overexpression of *Ch FatB2*, a thioesterase cDNA from *Cuphea hookeriana*. Plant J 9:167–172

Dudley JW, Dijkhuizen A, Paul C, Coates ST, Rocheford TR (2004) Effects of random-mating on marker-QTL associations in the cross of the Illinois High-Protein x Illinois Low Protein maize strains. Crop Sci 44:1419–1428

Dudley JW, Clark D, Rocheford TR, LeDeaux JR (2007) Genetic analysis of corn grain chemical composition in the random mated 7 generation of the cross of generations 70 of IHP 9 ILP. Crop Sci 47:45–57

Hills MJ (1999) Improving oil functionality by tuning catalysis of thioesterase. Trends Plant Sci 4:421–422

Jing F, Cantu DC, Tvaruzkova J, Chipman JP, Nikolau BJ, Yandeau-Nelson MD, Reilly PJ (2011) Phylogenetic and experimental characterization of an acyl-ACP thioesterase family reveals significant diversity in enzymatic specificity and activity. BMC Biochem. doi:10.1186/1471-2091-12-44

Jones A, Davies HM, Voelker TA (1995) Palmitoyl-acyl carrier protein (ACP) thioesterase and the evolutionary origin of plant acyl-ACP thioesterases. Plant Cell 7:359–371

Kim J, Kim DN, Lee SH, Yoo S-H, Lee S (2009) Correlation of fatty acid composition of vegetable oils with rheological behaviour and oil uptake. Food Chem 118:398–402

Kinney AJ, Cahoon EB, Hitz WD (2002) Manipulating desaturase activities in transgenic crop plants. Biochem Soc Trans 30:1099–1103

Laurie CC, Chasalow SD, Ledeaux JR, McCarroll R, Bush D, Hauge B, Lai CQ, Clark D, Rocheford TR, Dudley JW (2004) The genetic architecture of response to long-term artificial selection for oil concentration in the maize kernel. Genetics 168:2141–2155

Leto KJ, Ulrich JF (2004) Corn plants and products with improved oil composition. US Patent 6770801

Li L, Li H, Li Q, Yang X, Zheng D, Warburton M, Chai Y, Zhang P, Guo Y, Yan J, Li J (2011) An 11-bp insertion in *Zea mays fatb* reduces the palmitic acid content of fatty acids in maize grain. PLoS One 6(9):e24699

Li H, Peng Z, Yang X, Wang W, Fu J, Wang J, Han Y, Chai Y, Guo T, Yang N, Liu J, Warburton ML, Cheng Y, Hao X, Zhang P, Zhao J, Liu Y, Wang G, Li J, Yan J (2013) Genome-wide association study dissects the genetic architecture of oil biosynthesis in maize kernels. Nat Genet 45:43–50

Livak KJ, Schmittgen TD (2001) Analysis of relative gene expression data using real-time quantitative PCR and the 2(-Delta Delta C(T)) Method. Methods 25:402–408

Lu H, Romero-Severson J, Bernardo R (2002) Chromosomal regions associated with segregation distortion in maize. Theor Appl Genet 105:622–628

Mangolin CA, de Souza Jr CL, Garcia AAF, Garcia AF, Sibov ST, de Souza AP (2004) Mapping QTLs for kernel oil content in a tropical maize population. Euphytica 137:251–259

Mayer KM, Shanklin J (2005) A structural model of the plant acyl–acyl carrier protein thioesterase FatB comprises two

helix/4-stranded sheet domains, the N-terminal domain containing residues that affect specificity and the C-terminal domain containing catalytic residues. J Biol Chem 280:3621–3627

Mayer KM, Shanklin J (2007) Identification of amino acid residues involved in substrate specificity of plant acyl-ACP thioesterases using a bioinformatics-guided approach. BMC Plant Biol 7:1. doi:10.1186/1471-2229-7-1

Nagel B (2005) Corn products and methods for their production. US Patent 6914176

Pirtle RM, Yoder DW, Huynh TT, Nampaisansuk M, Pirtle IL, Chapman KD (1999) Characterization of a palmitoyl-acyl carrier protein thioesterase (FatB1) in cotton. Plant Cell Physiol 40:155–163

Salas JJ, Ohlrogge JB (2002) Characterization of substrate specificity of plant FatA and FatB acyl-ACP thioesterases. Arch Biochem Biophy 403:25–34

Shen B-J (2006) Method for improving the carcass quality of an animal. US Patent 7008664

Shen B, Allen WB, Zheng P, Li C, Glassman K, Ranch J, Nubel D, Tarczynski MC (2010) Expression of ZmLEC1 and ZmWRI1 increases seed oil production in maize. Plant Physiol 153:980–987

Voelker TA, Worrell AC, Anderson L, Bleibaum J, Fan C, Hawkins DJ, Radke SE, Davies HM (1992) Fatty acid biosynthesis redirected to medium chains in transgenic oilseed plants. Science 257:72–74

Wang Y, Li J, Li Y, Wei M, Li X, Fu J (2010) QTL detection for grain oil and starch content and their associations in two connected $F_{2:3}$ populations in high-oil maize. Euphytica 174:239–252

Wang G, He QQ, Xu ZK, Song RT (2012a) High segregation distortion in maize B73 x teosinte crosses. Genet Mol Res 11:693–706

Wang S, Basten CJ, Zeng Z-B (2012b) Windows QTL Cartographer 2.5. Department of Statistics, North Carolina State University, Raleigh. (http://statgen.ncsu.edu/qtlcart/WQTLCart.htm)

Wassom JJ, Wong JC, Martinez E, King JJ, DeBaene J, Hotchkiss JR, Mikkilineni V, Bohn MO, Rocheford TR (2008a) QTL associated with maize kernel oil, protein, and starch concentrations; kernel mass; and grain yield in Illinois High Oil x B73 backcross-derived lines. Crop Sci 48:243–252

Wassom JJ, Mikkilineni V, Bohn MO, Rocheford TR (2008b) QTL for fatty acid composition of maize kernel oil in Illinois high oil × B73 backcross-derived lines. Crop Sci 48:69–78

White PJ, Weber EJ (2003) Lipids of the kernel. In: White PJ, Johnson LA (eds) Corn: chemistry and technology, vol 10, 2nd edn edn. American Association of Cereal Chemists Inc, St. Paul, pp 355–395

Willmot DB, Dudley JW, Rocheford TR, Bari A (2006) Effect of random mating on marker-QTL associations for grain quality traits in the cross of Illinois high oil × Illinois low oil. Maydica 51:187–199

Wright A (1995) A gene conditioning high oleic maize oil, *OLC1*. Maydica 40:85–88

Wu PZ, Li J, Wei Q, Zeng L, Chen YP, Li MR, Jiang HW, Wu GJ (2009) Cloning and functional characterization of an acyl–acyl carrier protein thioesterase (JcFATB1) from *Jatropha curcas*. Tree Physiol 29:1299–1305

Yan JB, Tang JH, Meng YJ, Ma XQ, Teng WT, Chander S, Li L, Li JS (2003) Genetic analysis of segregation distortion of molecular markers in maize F2 population. Yi Chuan Xue Bao 30:913–918

Yang X, Guo Y, Yan J, Zhang J, Song T, Rocheford T, Li J (2010) Major and minor QTL and epistasis contribute to fatty acid compositions and oil concentration in high-oil maize. Theor Appl Genet 120:665–678

Yang X, Ma H, Zhang P, Yan J, Guo Y, Song T, Li J (2012) Characterization of QTL for oil content in maize kernel. Theor Appl Genet 125:1169–1179

Yuan L, Nelson BA, Caryl G (1996) The catalytic cysteine and histidine in the plant acyl–acyl carrier protein thioesterases. J Biol Chem 271:3417–3419

Zhang P, Allen WB, Nagasawa N, Ching AS, Heppard EP, Li H, Hao X, Li X, Yang X, Yan J, Nagato Y, Sakai H, Shen B, Li J (2012) A transposable element insertion within *ZmGE2* gene is associated with increase in embryo to endosperm ratio in maize. Theor Appl Genet 125:1463–1471

Zheng P, Allen WB, Williams ME, Zhang S, Li J, Glassman K, Ranch J, Nubel D, Solawetz W, Bhattramakki D, Llaca V, Deschamps S, Zhong G-Y, Tarczynski MC, Shen B (2008) A phenylalanine in DGAT is a key determinant of oil content and composition in maize. Nat Genet 40:367–372